

From Quantum Mechanics to Materials Design

Volker Eyert

Center for Electronic Correlations and Magnetism
Institute of Physics, University of Augsburg

October 14, 2010



Outline

1 Quantum Mechanics

- Density Functional Theory
- Full-Potential ASW Method

2 „Materials Design“

Outline

1 Quantum Mechanics

- Density Functional Theory
- Full-Potential ASW Method

2 „Materials Design“



Outline

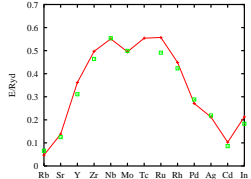
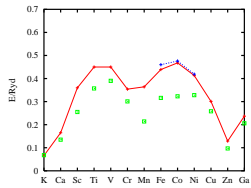
1 Quantum Mechanics

- Density Functional Theory
- Full-Potential ASW Method

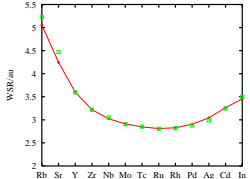
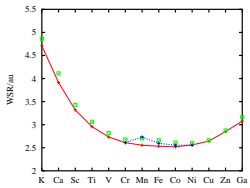
2 „Materials Design“

Calculated Electronic Properties

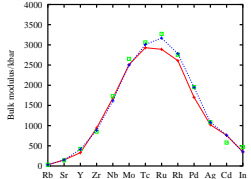
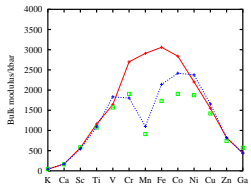
Moruzzi, Janak, Williams (IBM, 1978)



Cohesive Energies
 $\hat{=}$ Stability



Wigner-Seitz-Rad.
 $\hat{=}$ Volume

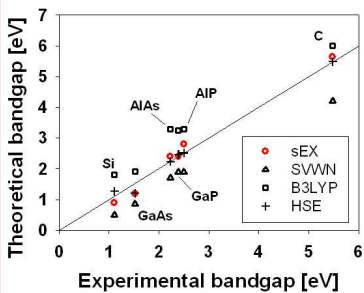


Compressibility
 $\hat{=}$ Hardness



Energy band structures from screened HF exchange

Si, AlP, AlAs, GaP, and GaAs



Experimental and
theoretical bandgap
properties

Shimazaki, Asai
JCP **132**, 224105 (2010)



Key Players

Hamiltonian (within Born-Oppenheimer approximation)

$$\begin{aligned} H &= H_{\text{el,kin}} + H_{\text{el-el}} + H_{\text{ext}} \\ &= \sum_i \left[-\frac{\hbar^2}{2m} \nabla_i^2 \right] + \frac{1}{2} \frac{e^2}{4\pi\epsilon_0} \sum_{\substack{i,j \\ j \neq i}} \frac{1}{|\mathbf{r}_i - \mathbf{r}_j|} + \sum_i v_{\text{ext}}(\mathbf{r}_i) \end{aligned}$$

where

$$\sum_i v_{\text{ext}}(\mathbf{r}_i) = \frac{1}{2} \frac{e^2}{4\pi\epsilon_0} \sum_{\substack{\mu,\nu \\ \mu \neq \nu}} \frac{Z_\mu Z_\nu}{|\mathbf{R}_\mu - \mathbf{R}_\nu|} - \frac{e^2}{4\pi\epsilon_0} \sum_\mu \sum_i \frac{Z_\mu}{|\mathbf{R}_\mu - \mathbf{r}_i|}$$

μ : ions with charge Z_μ , i : electrons

Key Players

Electron Density Operator

$$\hat{\rho}(\mathbf{r}) = \sum_{i=1}^N \delta(\mathbf{r} - \mathbf{r}_i) = \sum_{\alpha\beta} \chi_{\alpha}^{*}(\mathbf{r}) \chi_{\beta}(\mathbf{r}) \mathbf{a}_{\alpha}^{+} \mathbf{a}_{\beta}$$

χ_{α} : single particle state



Key Players

Electron Density Operator

$$\hat{\rho}(\mathbf{r}) = \sum_{i=1}^N \delta(\mathbf{r} - \mathbf{r}_i) = \sum_{\alpha\beta} \chi_{\alpha}^{*}(\mathbf{r}) \chi_{\beta}(\mathbf{r}) \mathbf{a}_{\alpha}^{+} \mathbf{a}_{\beta}$$

χ_{α} : single particle state

Electron Density

$$\rho(\mathbf{r}) = \langle \Psi | \hat{\rho}(\mathbf{r}) | \Psi \rangle = \sum_{\alpha} |\chi_{\alpha}(\mathbf{r})|^2 n_{\alpha}$$

$|\Psi\rangle$: many-body wave function, n_{α} : occupation number

Normalization: $N = \int d^3\mathbf{r} \rho(\mathbf{r})$

Key Players

Functionals

Universal Functional (**independent of ionic positions!**)

$$F = \langle \Psi | H_{el,kin} + H_{el-el} | \Psi \rangle$$

Functional due to External Potential:

$$\begin{aligned}\langle \Psi | H_{ext} | \Psi \rangle &= \langle \Psi | \sum_i v_{ext}(\mathbf{r}) \delta(\mathbf{r} - \mathbf{r}_i) | \Psi \rangle \\ &= \int d^3\mathbf{r} v_{ext}(\mathbf{r}) \rho(\mathbf{r})\end{aligned}$$



Authors

Pierre C. Hohenberg



Walter Kohn



Lu Jeu Sham



Hohenberg and Kohn, 1964: Theorems

1st Theorem

The external potential $v_{ext}(\mathbf{r})$ is determined, apart from a trivial constant, by the electronic ground state density $\rho(\mathbf{r})$.

2nd Theorem

The total energy functional $E[\rho]$ has a minimum equal to the ground state energy at the ground state density.



Hohenberg and Kohn, 1964: Theorems

1st Theorem

The external potential $v_{ext}(\mathbf{r})$ is determined, apart from a trivial constant, by the electronic ground state density $\rho(\mathbf{r})$.

2nd Theorem

The total energy functional $E[\rho]$ has a minimum equal to the ground state energy at the ground state density.

Nota bene

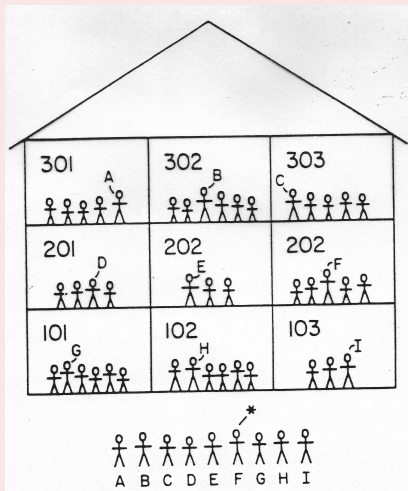
Both theorems are formulated for the ground state!

- Zero temperature!
- No excitations!



Levy, Lieb, 1979-1983: Constrained Search

Percus-Levy partition



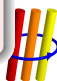
Levy, Lieb, 1979-1983: Constrained Search

Variational principle

$$\begin{aligned}E_0 &= \inf_{|\Psi\rangle} \langle \Psi | H | \Psi \rangle \\&= \inf_{|\Psi\rangle} \langle \Psi | H_{el,kin} + H_{el-el} + H_{ext} | \Psi \rangle \\&= \inf_{\rho(\mathbf{r})} \left[\inf_{|\Psi\rangle \in S(\rho)} \langle \Psi | H_{el,kin} + H_{el-el} | \Psi \rangle + \int d^3\mathbf{r} v_{ext}(\mathbf{r})\rho(\mathbf{r}) \right] \\&=: \inf_{\rho(\mathbf{r})} \left[F_{LL}[\rho] + \int d^3\mathbf{r} v_{ext}(\mathbf{r})\rho(\mathbf{r}) \right] = \inf_{\rho(\mathbf{r})} E[\rho]\end{aligned}$$

$S(\rho)$: set of all wave functions leading to density ρ

$F_{LL}[\rho]$: Levy-Lieb functional



Levy, Lieb, 1979-1983: Constrained Search

Levy-Lieb functional

$$\begin{aligned}
 F_{LL}[\rho] &= \inf_{|\Psi\rangle \in S(\rho)} \langle \Psi | H_{el,kin} + H_{el-el} | \Psi \rangle \\
 &= \underbrace{T[\rho] + W_{xc}[\rho]}_{G[\rho]} + \frac{1}{2} \frac{e^2}{4\pi\epsilon_0} \int d^3r \int d^3r' \frac{\rho(\mathbf{r})\rho(\mathbf{r}')}{|\mathbf{r}-\mathbf{r}'|} \\
 &= G[\rho] + \frac{1}{2} \frac{e^2}{4\pi\epsilon_0} \int d^3r \int d^3r' \frac{\rho(\mathbf{r})\rho(\mathbf{r}')}{|\mathbf{r}-\mathbf{r}'|}
 \end{aligned}$$

Functionals

- Kinetic energy funct.: $T[\rho]$ not known!
- Exchange-correlation energy funct.: $W_{xc}[\rho]$ not known!
- Hartree energy funct.: $\frac{1}{2} \frac{e^2}{4\pi\epsilon_0} \int d^3r \int d^3r' \frac{\rho(\mathbf{r})\rho(\mathbf{r}')}{|\mathbf{r}-\mathbf{r}'|}$ known!



Kohn and Sham, 1965: Single-Particle Equations

Ansatz

- ① use different splitting of the functional $G[\rho]$

$$T[\rho] + W_{xc}[\rho] = G[\rho] \stackrel{!}{=} T_0[\rho] + E_{xc}[\rho]$$

- ② reintroduce single-particle wave functions

Imagine: non-interacting electrons with same density

- Density: $\rho(\mathbf{r}) = \sum_{\alpha}^{occ} |\chi_{\alpha}(\mathbf{r})|^2$ known!
- Kinetic energy funct.:
 $T_0[\rho] = \sum_{\alpha}^{occ} \int d^3\mathbf{r} \chi_{\alpha}^*(\mathbf{r}) \left[-\frac{\hbar^2}{2m} \nabla^2 \right] \chi_{\alpha}(\mathbf{r})$ known!
- Exchange-correlation energy funct.: $E_{xc}[\rho]$ not known!



Kohn and Sham, 1965: Single-Particle Equations

Euler-Lagrange Equations (Kohn-Sham Equations)

$$\frac{\delta E[\rho]}{\delta \chi_\alpha^*(\mathbf{r})} - \varepsilon_\alpha \chi_\alpha(\mathbf{r}) = \left[-\frac{\hbar^2}{2m} \nabla^2 + v_{\text{eff}}(\mathbf{r}) - \varepsilon_\alpha \right] \chi_\alpha(\mathbf{r}) \stackrel{!}{=} 0$$

- Effective potential: $v_{\text{eff}}(\mathbf{r}) := v_{\text{ext}}(\mathbf{r}) + v_H(\mathbf{r}) + v_{xc}(\mathbf{r})$
- Exchange-correlation potential: not known!

$$v_{xc}(\mathbf{r}) := \frac{\delta E_{xc}[\rho]}{\delta \rho}$$

- „Single-particle energies“:
 ε_α (Lagrange-parameters, orthonormalization)



Kohn and Sham, 1965: Local Density Approximation

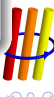
Be Specific!

- Approximate exchange-correlation energy functional

$$E_{xc}[\rho] = \int \rho(\mathbf{r}) \varepsilon_{xc}(\rho(\mathbf{r})) d^3\mathbf{r}$$

- Exchange-correlation energy density $\varepsilon_{xc}(\rho(\mathbf{r}))$
 - depends on **local** density only!
 - is calculated from **homogeneous**, interacting electron gas
- Exchange-correlation potential

$$v_{xc}(\rho(\mathbf{r})) = \left[\frac{\partial}{\partial \rho} \{ \rho \varepsilon_{xc}(\rho) \} \right]_{\rho=\rho(\mathbf{r})}$$

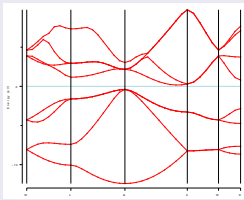


Kohn and Sham, 1965: Local Density Approximation

Limitations and Beyond

- LDA **exact** for homogeneous electron gas (within QMC)
- **Spatial variation of ρ ignored**
 - include $\nabla\rho(\mathbf{r}), \dots$
 - Generalized Gradient Approximation (GGA)
- **Self-interaction cancellation in $v_{Hartree} + v_x$ violated**

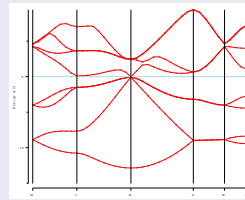
Si



Bandgaps

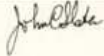
- Si, exp: 1.11 eV
- Si, GGA: 0.57 eV
- Ge, exp: 0.67 eV
- Ge, GGA: 0.09 eV

Ge



Muffin-Tin Approximation

John C. Slater

A handwritten signature of John C. Slater's name in black ink.

Full Potential

$$v_\sigma(\mathbf{r}) : \begin{cases} \text{spherical symmetric near nuclei} \\ \text{flat outside the atomic cores} \end{cases}$$

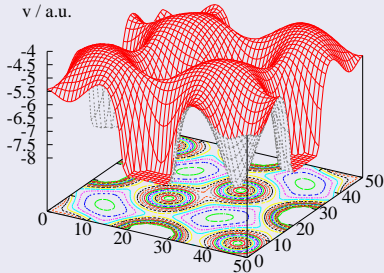
Muffin-Tin Approximation

$$v_\sigma^{MT}(\mathbf{r}) = \begin{cases} \text{spherical symmetric in spheres} \\ \text{constant in interstitial region} \end{cases}$$


Muffin-Tin Approximation

Full Potential

(FeS₂)



Muffin-Tin Potential

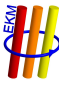


Muffin-Tin Approximation

Wave Function

- ① solve Schrödinger's eq.
→ **partial waves**
- ② match partial waves
→ basis functions,
„augmented“ partial waves
- ③ use to expand
→ **wave function**

Muffin-Tin Potential



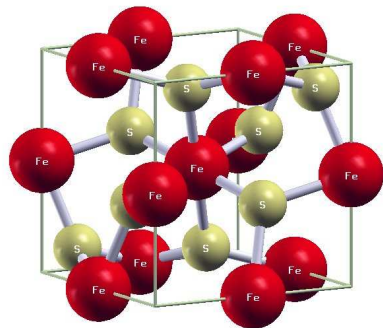
Muffin-Tin Approximation

Flavors

- Muffin-Tin Approximation: touching spheres
- Atomic Sphere Approximation: space-filling spheres
 - interstitial region formally removed
 - only numerical functions in spheres
 - minimal basis set (s, p, d)
 - very high computational efficiency → $\mathcal{O}(\text{ASA})$ speed!!!
 - makes potential more realistic
 - systematic error in total energybad!



Iron Pyrite: FeS₂



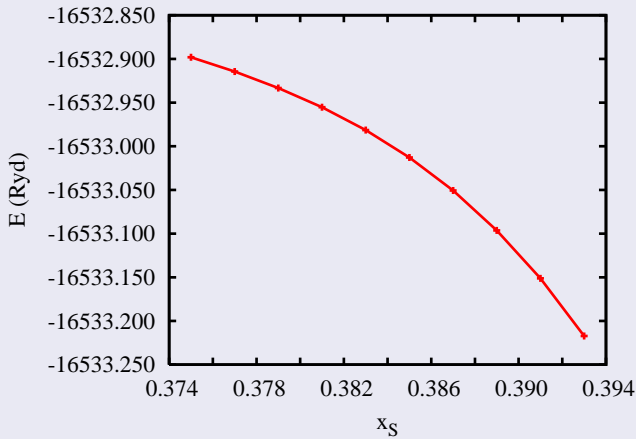
Pyrite

- $\bar{P}a\bar{3}$ (T_h^6)
- $a = 5.4160 \text{ \AA}$
- “NaCl structure” sublattices occupied by
 - iron atoms
 - sulfur pairs
- sulfur pairs $\parallel \langle 111 \rangle$ axes
- $x_S = 0.38484$
- rotated FeS₆ octahedra



FeS₂: Structure Optimization

ASA⁺ Code



Basic Principles of the Full-Potential ASW Method

Steps to be Taken

- remove total energy error due to overlap of atomic spheres
 - reintroduce non-overlapping muffin-tin spheres
 - restore interstitial region



Basic Principles of the Full-Potential ASW Method

Steps to be Taken

- remove total energy error due to overlap of atomic spheres
 - reintroduce non-overlapping muffin-tin spheres
 - restore interstitial region
- find representation of electron density and full potential
 - inside muffin-tin spheres
 - in the interstitial region



Basic Principles of the Full-Potential ASW Method

Steps to be Taken

- remove total energy error due to overlap of atomic spheres
 - reintroduce non-overlapping muffin-tin spheres
 - restore interstitial region
- find representation of electron density and full potential
- find representation of products of the wave function
 - inside muffin-tin spheres
 - in the interstitial region



Basic Principles of the Full-Potential ASW Method

Steps to be Taken

- remove total energy error due to overlap of atomic spheres
 - reintroduce non-overlapping muffin-tin spheres
 - restore interstitial region
- find representation of electron density and full potential
- find representation of products of the wave function
- find representation of products of the basis functions
 - inside muffin-tin spheres
 - in the interstitial region



Basic Principles of the Full-Potential ASW Method

Steps to be Taken

- remove total energy error due to overlap of atomic spheres
 - reintroduce non-overlapping muffin-tin spheres
 - restore interstitial region
- find representation of electron density and full potential
- find representation of products of the wave function
- find representation of products of the basis functions
 - inside muffin-tin spheres
 - use spherical-harmonics expansions
 - in the interstitial region



Basic Principles of the Full-Potential ASW Method

Steps to be Taken

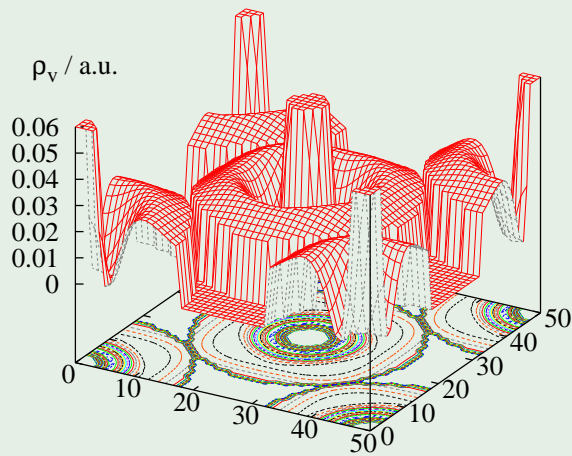
- remove total energy error due to overlap of atomic spheres
 - reintroduce non-overlapping muffin-tin spheres
 - restore interstitial region
- find representation of electron density and full potential
- find representation of products of the wave function
- find representation of products of the basis functions
 - inside muffin-tin spheres
 - use spherical-harmonics expansions
 - in the interstitial region
 - no exact spherical-wave representation available!



From Wave Functions to Electron Density

Density inside MT-Spheres

(AI)



From Wave Functions to Electron Density

Products of Spherical Waves in Interstitial Region

- expand in **spherical waves**
 - would be efficient
 - coefficients/integrals not known analytically
 - Methfessel, 1988:
match values and slopes at MT-sphere surfaces



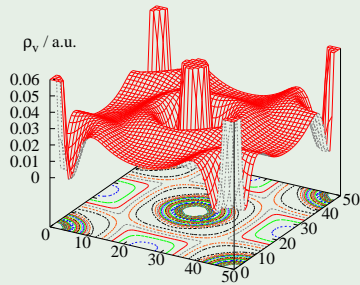
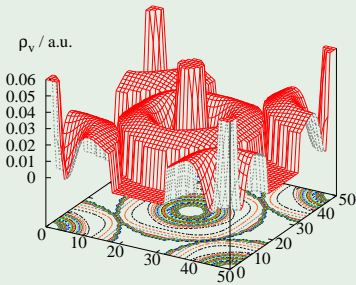
From Wave Functions to Electron Density

Products of Spherical Waves in Interstitial Region

- expand in **spherical waves**
 - match values and slopes at **MT-sphere** surfaces

Density from Value/Slope Matching at MT-Radii

(AI)



Comparison of Approaches

Ole K. Andersen

1975

- ASA geometry used for basis functions
→ minimal basis set
- ASA geometry used for density and potential
→ error in total energy

good!

bad!



Comparison of Approaches

Ole K. Andersen

1975

- ASA geometry used for basis functions
→ minimal basis set
- ASA geometry used for density and potential
→ error in total energy

good!

bad!

Michael S. Methfessel

1988

- MT geometry used for density and potential
→ accurate total energy
- MT geometry used for basis functions
→ large basis set

good!

bad!



Comparison of Approaches

Ole K. Andersen 1975

- ASA geometry used for basis functions good!
- ASA geometry used for density and potential bad!

Michael S. Methfessel 1988

- MT geometry used for density and potential good!
- MT geometry used for basis functions bad!

present approach 2006

- ASA geometry used for basis functions
→ minimal basis set → $\mathcal{O}(\text{ASA})$ speed great!
- MT geometry used for density and potential
→ accurate total energy great!

Implementation: Augmented Spherical Wave Method

0th Generation ASW (Williams, Kübler, Gelatt, 1970s)

PRB **19**, 6094 (1979)

1st Generation (VE, 1990s)

- new implementation (accurate, stable, portable)
VE, Int. J. Quantum Chem. **77**, 1007 (2000)
VE, Lect. Notes Phys. **719** (Springer, 2007)
- xAnderson convergence acceleration scheme
VE, J. Comput. Phys. **124**, 271 (1996)
- all LDA- and GGA-parametrizations
- still based on atomic-sphere approximation
VE, Höck, PRB **57**, 12727 (1998)

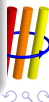
Implementation: Augmented Spherical Wave Method

2nd Generation ASW (VE, 2000s)

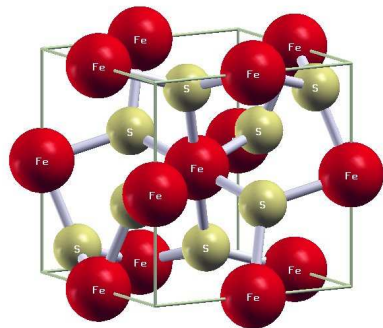
- based on 1st generation code
- full-potential ASW method
 - electron densities, spin densities
 - electric field gradients
 - elastic properties, phonon spectra
- optical properties
 - based on linear-response theory
 - direct calculation of $\Re\sigma$ and $\Im\sigma$
 - no Kramers-Kronig relations needed
- transport properties, thermoelectrics
- LDA+U method
 - all „flavors“ for double-counting terms (AMF, FLL, DFT)

at $\mathcal{O}(\text{ASA})$ speed!

VE, Lect. Notes Phys. (2nd ed., Springer, 2011)



Iron Pyrite: FeS₂



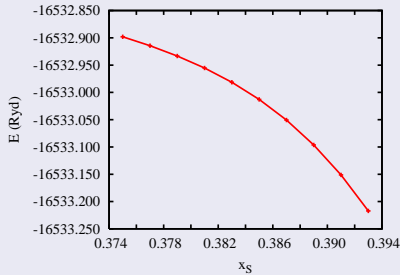
Pyrite

- $\bar{P}a\bar{3}$ (T_h^6)
- $a = 5.4160 \text{ \AA}$
- “NaCl structure” sublattices occupied by
 - iron atoms
 - sulfur pairs
- sulfur pairs $\parallel \langle 111 \rangle$ axes
- $x_S = 0.38484$
- rotated FeS₆ octahedra



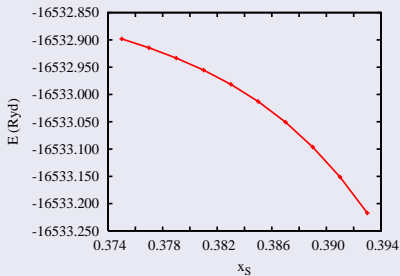
FeS₂: Structure Optimization

ASA⁺ Code

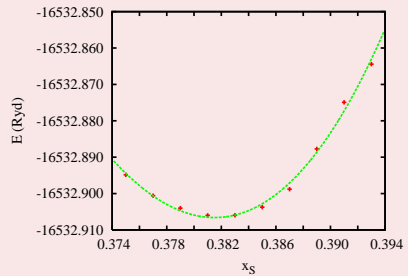


FeS₂: Structure Optimization

ASA⁺ Code



Full-Potential Code

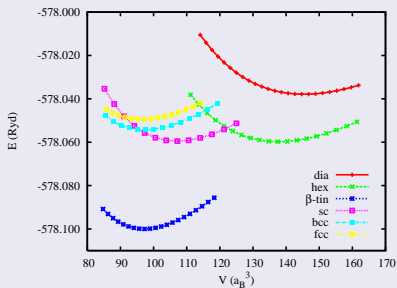


at $\mathcal{O}(\text{ASA})$ speed!



Phase Stability in Silicon

ASA⁺ Code

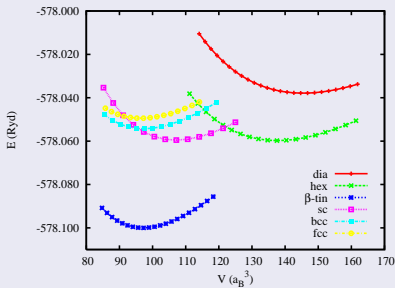


Bad

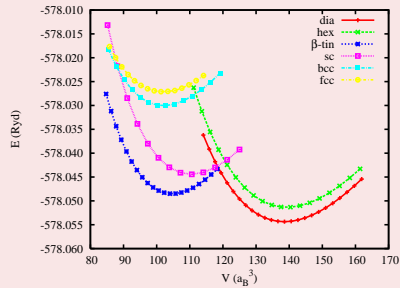
- β -tin structure most stable # nature (diamond structure)

Phase Stability in Silicon

ASA⁺ Code



Full-Potential Code



New!

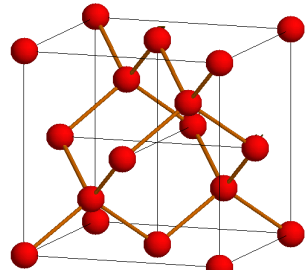
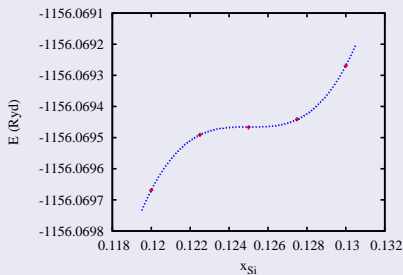
at $\mathcal{O}(\text{ASA})$ speed!

- diamond structure most stable
- pressure induced phase transition to β -tin structure



LTO(Γ)-Phonon in Silicon

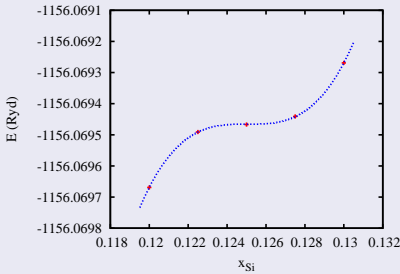
ASA⁺ Code



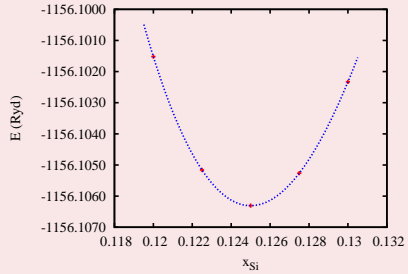
Bad

- no stable Si position # nature



LTO(Γ)-Phonon in SiliconASA⁺ Code

Full-Potential Code



New!

at $\mathcal{O}(\text{ASA})$ speed!

- phonon frequency: $f_{\text{calc}} = 15.34 \text{ THz}$ ($f_{\text{exp}} = 15.53 \text{ THz}$)



Outline

1 Quantum Mechanics

- Density Functional Theory
- Full-Potential ASW Method

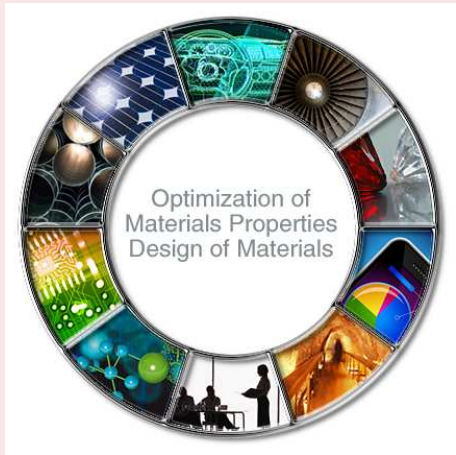
2 „Materials Design“



Industrial Applications

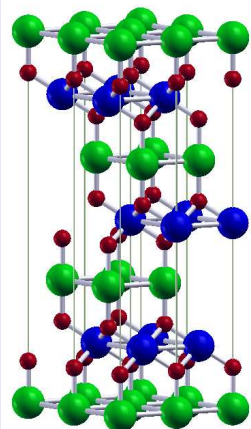
Computational Materials Engineering

- Automotive
- Energy & Power Generation
- Aerospace
- Steel & Metal Alloys
- Glass & Ceramics
- Electronics
- Display & Lighting
- Chemical & Petrochemical
- Drilling & Mining



Delafoossites: ABO_2

Delafoosite Structure



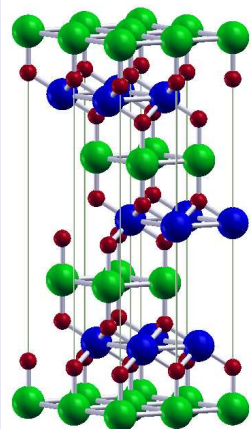
Building Blocks

- rhombohedral lattice
- triangular A -atom layers
- BO_2 sandwich layers
- B-atoms octahedrally coordinated
- linear $\text{O}-\text{A}-\text{O}$ bonds



Delafoossites: ABO_2

Delafoosite Structure



Building Blocks

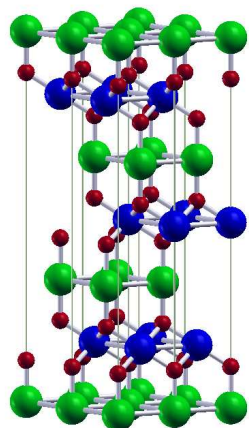
- rhombohedral lattice
- triangular A -atom layers
- BO_2 sandwich layers
- B-atoms octahedrally coordinated
- linear $\text{O}-\text{A}-\text{O}$ bonds

Issues

- dimensionality
- geometric frustration
- play chemistry

Delafoossites: ABO_2

Delafoosite Structure



Prototype Materials

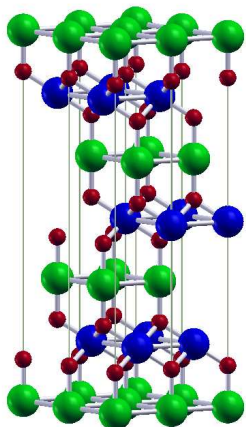
- CuFeO_2 , CuCrO_2
- CuCoO_2 , CuRhO_2
- CuAlO_2 , CuGaO_2 , CuInO_2 , ...
- PdCrO_2 , PdCoO_2 , PdRhO_2 , PtCoO_2

Properties

- semiconductors, AF interactions, (distorted) triangular
- non-magn. semicond., thermopower
- wide-gap semicond., p-type TCO
- very good metals, high anisotropy

Delafoossites: ABO_2

Delafoosite Structure



Prototype Materials

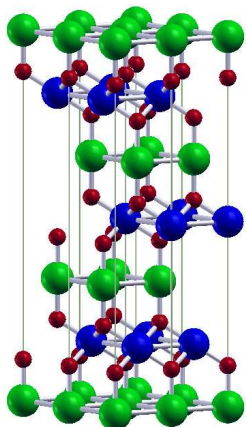
- CuFeO_2 , CuCrO_2
- CuCoO_2 , CuRhO_2
- CuAlO_2 , CuGaO_2 , CuInO_2 , ...
- PdCrO_2 , PdCoO_2 , PdRhO_2 , PtCoO_2

Properties

- semiconductors, AF interactions,
(distorted) triangular
- non-magn. semicond., thermopower
- wide-gap semicond., p-type TCO
- very good metals, high anisotropy

Delafoossites: ABO_2

Delafoosite Structure



Prototype Materials

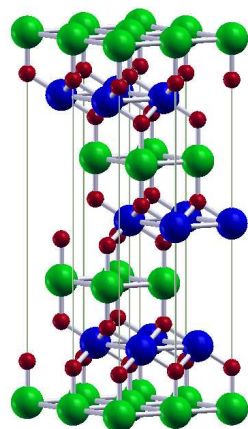
- CuFeO_2 , CuCrO_2
- CuCoO_2 , CuRhO_2
- CuAlO_2 , CuGaO_2 , CuInO_2 , ...
- PdCrO_2 , PdCoO_2 , PdRhO_2 , PtCoO_2

Properties

- semiconductors, AF interactions, (distorted) triangular
- non-magn. semicond., thermopower
- wide-gap semicond., p-type TCO
- very good metals, high anisotropy

Delafoossites: ABO_2

Delafoosite Structure



Prototype Materials

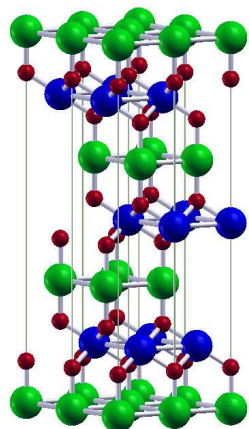
- CuFeO_2 , CuCrO_2
- CuCoO_2 , CuRhO_2
- CuAlO_2 , CuGaO_2 , CuInO_2 , ...
- PdCrO_2 , PdCoO_2 , PdRhO_2 , PtCoO_2

Properties

- semiconductors, AF interactions, (distorted) triangular
- non-magn. semicond., thermopower
- wide-gap semicond., p-type TCO
- very good metals, high anisotropy

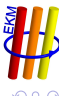
PdCoO₂ and PtCoO₂

Delafoseite Structure



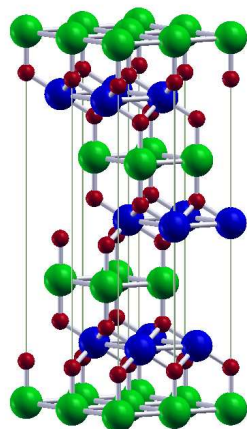
Experimental Results

- very low resistivity
- anisotropy ratio ≈ 200
- PES: only Pd 4d states at E_F
- PES/IPES: E_F in shallow DOS minimum
 - high thermopower on doping?



PdCoO₂ and PtCoO₂

Delafoseite Structure



Experimental Results

- very low resistivity
- anisotropy ratio ≈ 200
- PES: only Pd 4d states at E_F
- PES/IPES: E_F in shallow DOS minimum
 - high thermopower on doping?

Open Issues

role of Pd 4d, Co 3d, and O 2p orbitals?

Structure Optimization in PdCoO₂

Structural Data

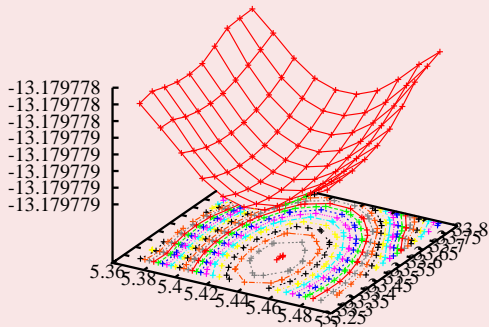
experiment

- $a = 2.83 \text{ \AA}$
- $c = 17.743 \text{ \AA}$
- $z_0 = 0.1112$

theory

- $a = 2.8767 \text{ \AA}$
- $c = 17.7019 \text{ \AA}$
- $z_0 = 0.1100$

Total energy surface

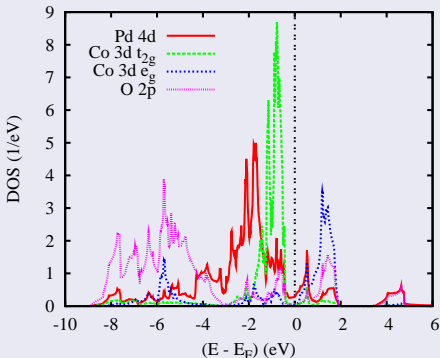


VE, R. Frésard, A. Maignan, Chem. Mat. **20**, 2370 (2008)



Electronic Properties of PdCoO₂

Partial Densities of States



Results

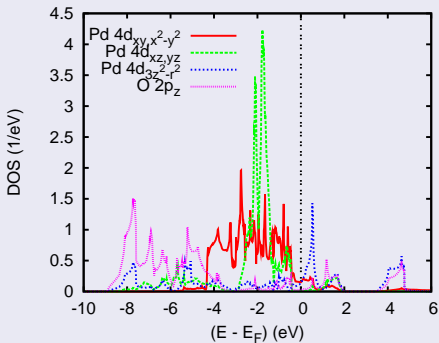
- Co 3d-O 2p hybridization
- CoO₆ octahedra:
 $\text{Co } 3d \Rightarrow t_{2g} \text{ and } e_g$
- Co 3d⁶ (Co³⁺) LS
- Pd 4d⁹ (Pd¹⁺)
- Co 3d, O 2p: very small DOS at E_F

VE, R. Frésard, A. Maignan, Chem. Mat. **20**, 2370 (2008)



Electronic Properties of PdCoO₂

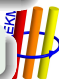
Partial Densities of States



Results

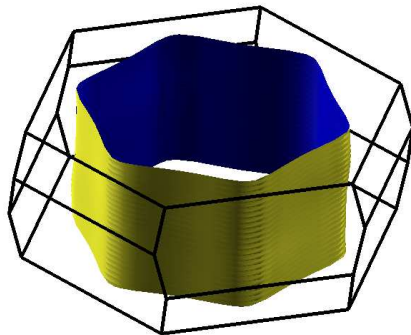
- broad Pd d_{xy,x^2-y^2} bands
 - short in-plane Pd-Pd distance
- non-bonding Pd $d_{xz,yz}$ bands
- strong Pd $4d_{3z^2-r^2}$ -O $2p$ hybridization
- states at E_F:
Pd d_{xy,x^2-y^2} , $d_{3z^2-r^2}$

VE, R. Frésard, A. Maignan, Chem. Mat. **20**, 2370 (2008)



Electronic Properties of PdCoO₂

Fermi Surface



Results

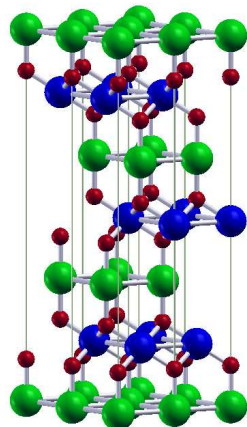
- quasi-2D
- single band crossing E_F
- but: bands below E_F disperse along Γ -A

VE, R. Frésard, A. Maignan, Chem. Mat. **20**, 2370 (2008)



CuFeO₂

Delafoseite Structure



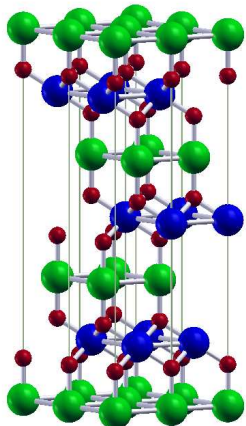
Basics

- semiconductor
- AF interactions
- triangular lattice



CuFeO₂

Delafoseite Structure



Basics

- semiconductor
- AF interactions
- triangular lattice

Open Issues

- frustration vs. long-range order
- role of Cu 3d orbitals?
- role of Fe 3d and O 2p orbitals?

CuFeO₂

Previous Neutron Data

- $T_{N_1} = 16\text{ K}$, $T_{N_2} = 11\text{ K}$
- $\Theta_{CW} = -90\text{ K}$
- magnetic supercells
- no structural distortion
- $m_{\text{Fe}^{3+}} = 4.4\mu_B$

CuFeO₂

Previous Neutron Data

- $T_{N_1} = 16\text{ K}$, $T_{N_2} = 11\text{ K}$
- $\Theta_{CW} = -90\text{ K}$
- magnetic supercells
- no structural distortion
- $m_{\text{Fe}^{3+}} = 4.4\mu_B$

Band Calculations

- rhombohedral structure
- $m_{\text{Fe}} = 0.9\mu_B$, $m_{\text{Fe}} = 3.8\mu_B$
- $E_g = 0$ in LDA, GGA
- \ddagger PES, XES



CuFeO₂

Previous Neutron Data

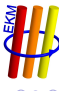
- $T_{N_1} = 16\text{ K}$, $T_{N_2} = 11\text{ K}$
- $\Theta_{CW} = -90\text{ K}$
- magnetic supercells
- no structural distortion
- $m_{\text{Fe}^{3+}} = 4.4\mu_B$

Band Calculations

- rhombohedral structure
- $m_{\text{Fe}} = 0.9\mu_B$, $m_{\text{Fe}} = 3.8\mu_B$
- $E_g = 0$ in LDA, GGA
- \ddagger PES, XES

New Neutron Data

- magnetic supercells
- monoclinic structure below 4K



CuFeO₂

Previous Neutron Data

- $T_{N_1} = 16\text{ K}$, $T_{N_2} = 11\text{ K}$
- $\Theta_{CW} = -90\text{ K}$
- magnetic supercells
- no structural distortion
- $m_{\text{Fe}^{3+}} = 4.4\ \mu_B$

New Neutron Data

- magnetic supercells
- monoclinic structure below 4 K

Band Calculations

- rhombohedral structure
- $m_{\text{Fe}} = 0.9\ \mu_B$, $m_{\text{Fe}} = 3.8\ \mu_B$
- $E_g = 0$ in LDA, GGA
- \ddagger PES, XES

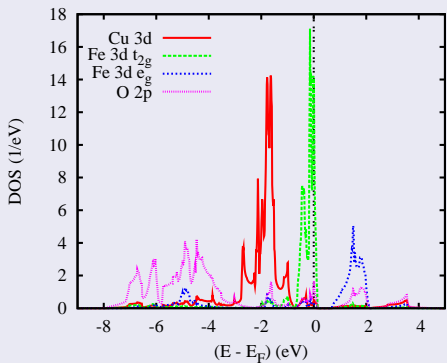
Open Issues

- spin-state of Fe?
- influence of monoc. structure?



Electronic Properties of CuFeO₂

Partial Densities of States



Results

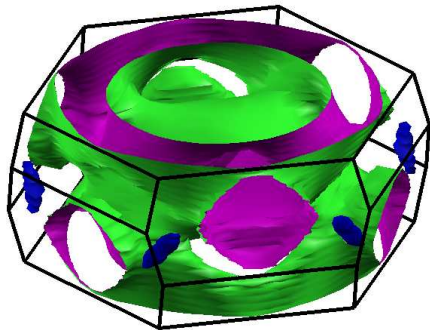
- Fe 3d-O 2p hybridization
- FeO₆ octahedra:
 $\text{Fe } 3d \Rightarrow t_{2g} \text{ and } e_g$
- Cu 4d¹⁰ (Cu¹⁺)
- Fe 3d t_{2g}
 - sharp peak at E_F

VE, R. Frésard, A. Maignan, PRB **78**, 052402 (2008)



Electronic Properties of CuFeO₂

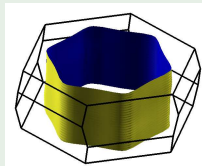
Fermi Surface



Results

- strongly 3D

FS PdCoO₂



VE, R. Frésard, A. Maignan, PRB **78**, 052402 (2008)



Magnetic Properties of CuFeO₂

Total Energies (mRyd/f.u.), Magn. Moms. (μ_B), Band Gaps (eV)

structure	magn. order	ΔE	m_{Fe}	m_{O}	E_g
rhomb.	spin-deg.	0.0			-
rhomb.	ferro (LS)	-16.7	1.03	-0.02	-
rhomb.	ferro (IS)	-12.0	2.02	-0.02	-
rhomb.	ferro (HS)	-19.2	3.73	0.21	-

VE, R. Frésard, A. Maignan, PRB **78**, 052402 (2008)

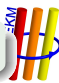


Magnetic Properties of CuFeO₂

Total Energies (mRyd/f.u.), Magn. Moms. (μ_B), Band Gaps (eV)

structure	magn. order	ΔE	m_{Fe}	m_{O}	E_g
rhomb.	spin-deg.	0.0			-
rhomb.	ferro (LS)	-16.7	1.03	-0.02	-
rhomb.	ferro (IS)	-12.0	2.02	-0.02	-
rhomb.	ferro (HS)	-19.2	3.73	0.21	-
monoc.	spin-deg.	-6.0			-
monoc.	ferro (LS)	-21.5	1.04	-0.02	-
monoc.	ferro (IS)	-19.0	2.08	-0.02	-
monoc.	ferro (HS)	-32.0	3.62	0.19	-

VE, R. Frésard, A. Maignan, PRB **78**, 052402 (2008)

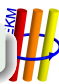


Magnetic Properties of CuFeO₂

Total Energies (mRyd/f.u.), Magn. Moms. (μ_B), Band Gaps (eV)

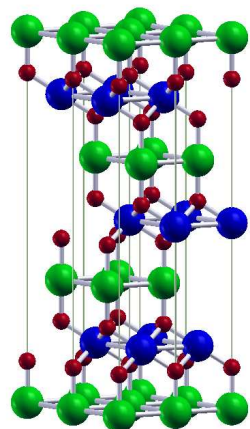
structure	magn. order	ΔE	m_{Fe}	m_0	E_g
rhomb.	spin-deg.	0.0			-
rhomb.	ferro (LS)	-16.7	1.03	-0.02	-
rhomb.	ferro (IS)	-12.0	2.02	-0.02	-
rhomb.	ferro (HS)	-19.2	3.73	0.21	-
monoc.	spin-deg.	-6.0			-
monoc.	ferro (LS)	-21.5	1.04	-0.02	-
monoc.	ferro (IS)	-19.0	2.08	-0.02	-
monoc.	ferro (HS)	-32.0	3.62	0.19	-
monoc.	antiferro	-46.0	± 3.72	± 0.08	0.05

VE, R. Frésard, A. Maignan, PRB **78**, 052402 (2008)



CuRhO₂

Delafoseite Structure

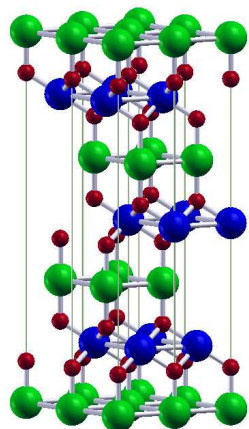


Experimental Findings

- semiconductor
- high thermopower on hole doping
 - $\text{Rh}^{3+} \longrightarrow \text{Mg}^{2+}$ up to 12%
- high T -independent power factor

CuRhO₂

Delafoseite Structure



Experimental Findings

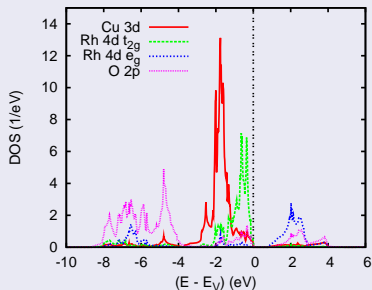
- semiconductor
- high thermopower on hole doping
 - $\text{Rh}^{3+} \longrightarrow \text{Mg}^{2+}$ up to 12%
- high T -independent power factor

Open Issues

- origin of high thermopower
- role of Cu 3d orbitals?
- role of Rh 4d and O 2p orbitals?

Electronic Properties of CuRhO₂

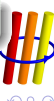
Partial Densities of States



Results

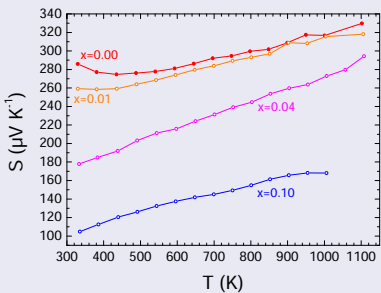
- Rh 4d-O 2p hybridization
- RhO₆ octahedra:
 $\text{Rh } 4d \Rightarrow t_{2g} \text{ and } e_g$
- $E_g \approx 0.75 \text{ eV}$
- Cu 4d¹⁰ (Cu^{1+})
- electronic structure:
strongly 3D

A. Maignan, VE et al., PRB **80**, 115103 (2009)

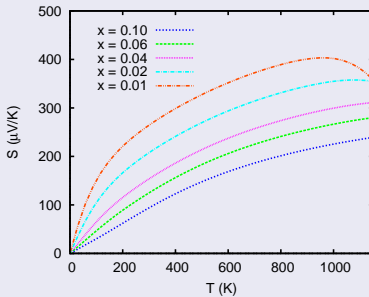


Thermoelectric Power of CuRh_{1-x}Mg_xO₂

Experiment



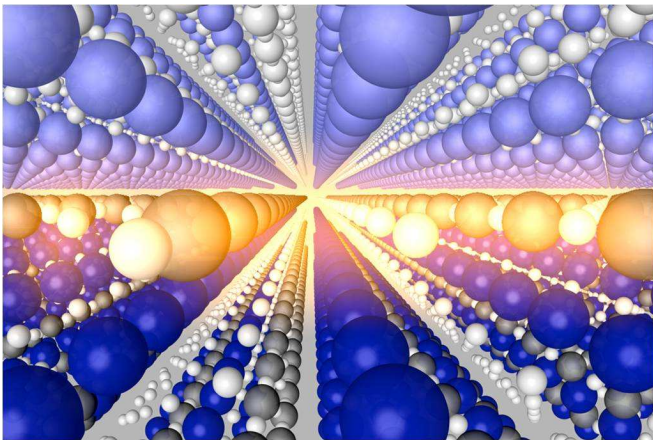
Theory: S_{xx}



A. Maignan, VE et al., PRB **80**, 115103 (2009)

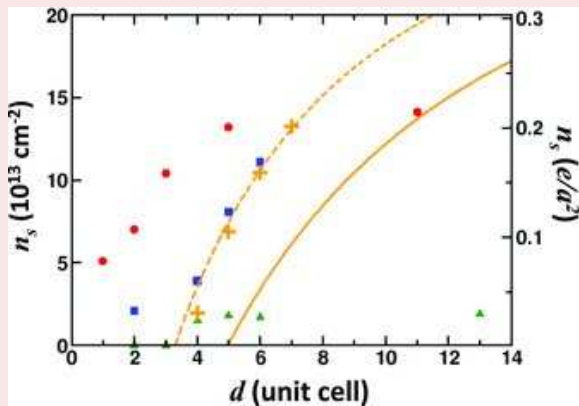


2D Electron Gas at LaAlO₃-SrTiO₃ Interface



2D Electron Gas at LaAlO₃-SrTiO₃ Interface

Insulator-Metal Transition



Chen, Kolpak, Ismail-Beigi, Adv. Mater. **22**, 2881 (2010)

Slab Calculations for the LaAlO₃-SrTiO₃ Interface



Structural setup of calculations

- central region: 5 layers SrTiO₃, TiO₂-terminated
- sandwiches: 2 to 5 layers LaAlO₃, AlO₂ surface
- vacuum region $\approx 20 \text{ \AA}$
- inversion symmetry
- lattice constant of SrTiO₃ from GGA (3.944 Å)



Slab Calculations for the LaAlO₃-SrTiO₃ Interface



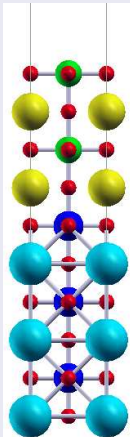
Calculational method

- Vienna Ab Initio Simulation Package (VASP)
- GGA-PBE
- Steps:
 - 1 optimization of SrTiO₃ lattice constant
 - 2 slab calculations
 - full relaxation of all atomic positions
 - $5 \times 5 \times 1$ \mathbf{k} -points
 - Γ -centered \mathbf{k} -mesh
 - Methfessel-Paxton BZ-integration

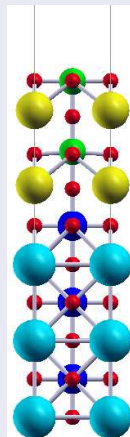


Slab Calculations for the LaAlO₃-SrTiO₃ Interface

Ideal



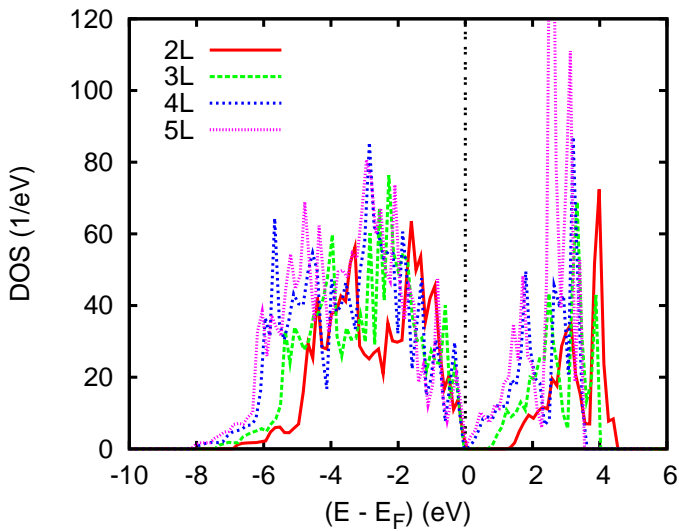
Optimized



Structural relaxation

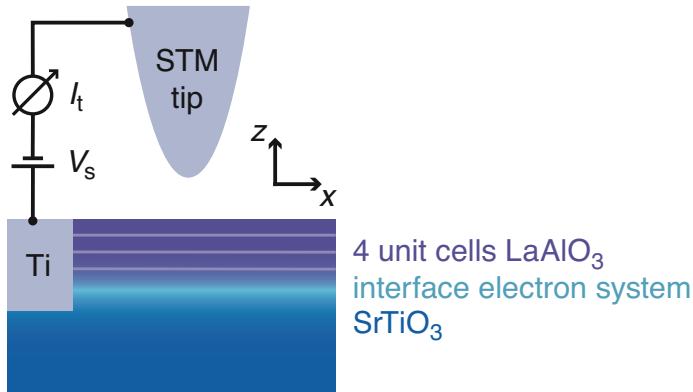
- AlO₂ surface layers
 - strong inward relaxation
 - weak buckling
- LaO layers
 - strong buckling
- AlO₂ subsurface layers
 - buckling
- TiO₂ interface layers
 - small outward relaxation

Slab Calculations for the LaAlO₃-SrTiO₃ Interface



Tunneling Spectroscopy of LaAlO₃-SrTiO₃ Interface

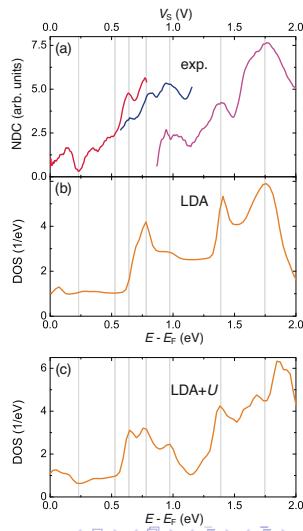
What is the origin of the 2-DEG?
Intrinsic mechanism or defect-doping?



M. Breitschaft *et al.*, PRB **81**, 153414 (2010)

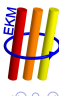
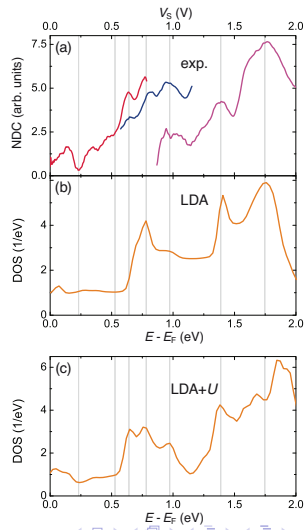
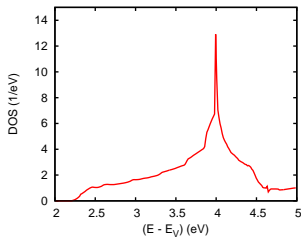
Tunneling Spectroscopy of LaAlO₃-SrTiO₃ Interface

- 4uc LaAlO₃ on SrTiO₃, tunneling data
- 4uc LaAlO₃ on SrTiO₃, LDA calculations, DOS of interface Ti
- 4uc LaAlO₃ on SrTiO₃, LDA+U calculations, DOS of interface Ti

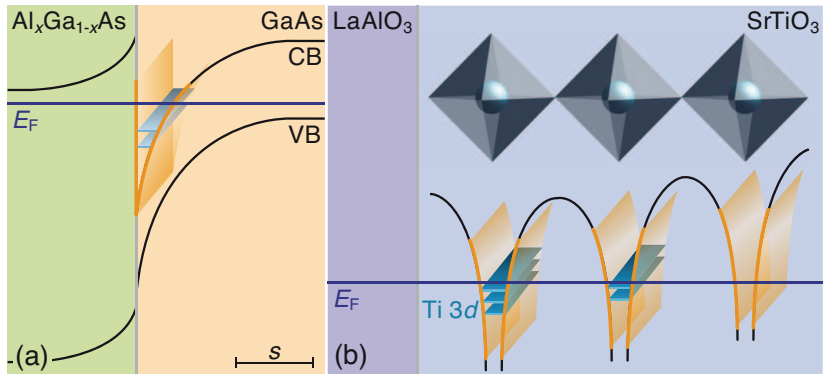


Tunneling Spectroscopy of LaAlO₃-SrTiO₃ Interface

- bulk SrTiO₃,
LDA calculations,
conduction band DOS



“2D Electron Liquid State” at LaAlO₃-SrTiO₃ Interface



M. Breitschaft *et al.*, PRB **81**, 153414 (2010)



Critical review of the Local Density Approximation

Limitations and Beyond

- Self-interaction cancellation in $v_{Hartree} + v_x$ violated
- Repair using exact Hartree-Fock exchange functional
→ class of hybrid functionals

- PBE0

$$E_{xc}^{PBE0} = \frac{1}{4}E_x^{HF} + \frac{3}{4}E_x^{PBE} + E_c^{PBE}$$

- HSE03, HSE06

$$E_{xc}^{HSE} = \frac{1}{4}E_x^{HF,sr,\mu} + \frac{3}{4}E_x^{PBE,sr,\mu} + E_x^{PBE,Ir,\mu} + E_c^{PBE}$$

based on decomposition of Coulomb kernel

$$\frac{1}{r} = S_\mu(r) + L_\mu(r) = \frac{\operatorname{erfc}(\mu r)}{r} + \frac{\operatorname{erf}(\mu r)}{r}$$

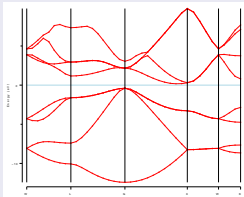


Critical review of the Local Density Approximation

Limitations and Beyond

- Self-interaction cancellation in $v_{Hartree} + v_x$ violated
- Repair using exact Hartree-Fock exchange functional
→ class of hybrid functionals

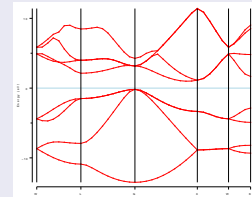
GGA



Si bandgap

- exp: 1.11 eV
- GGA: 0.57 eV
- HSE: 1.15 eV

HSE

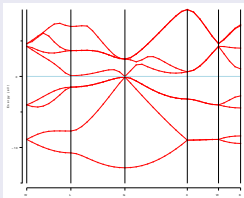


Critical review of the Local Density Approximation

Limitations and Beyond

- Self-interaction cancellation in $v_{Hartree} + v_x$ violated
- Repair using exact Hartree-Fock exchange functional
→ class of hybrid functionals

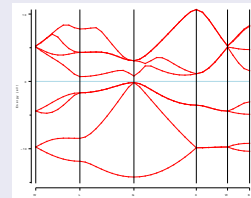
GGA



Ge bandgap

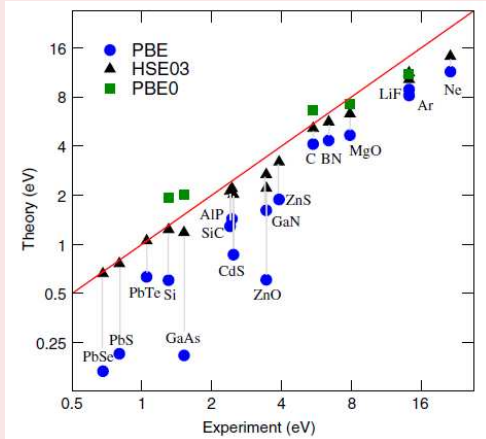
- exp: 0.67 eV
- GGA: 0.09 eV
- HSE: 0.66 eV

HSE



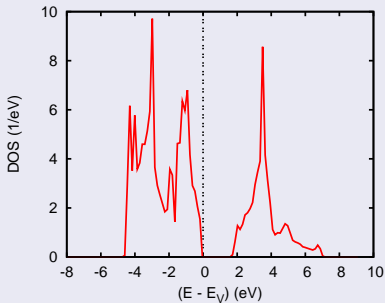
Critical review of the Local Density Approximation

Calculated vs. experimental bandgaps



SrTiO₃

GGA



Bandgap

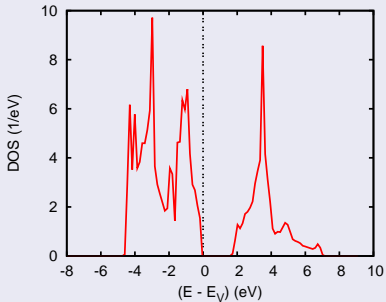
GGA: ≈ 1.6 eV,

exp.: 3.2 eV

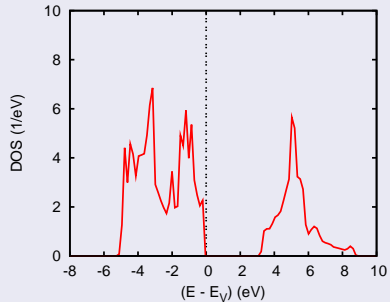


SrTiO₃

GGA



HSE



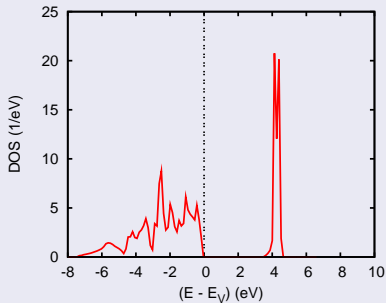
Bandgap

GGA: $\approx 1.6 \text{ eV}$, HSE: $\approx 3.1 \text{ eV}$, exp.: 3.2 eV



LaAlO₃

GGA



Bandgap

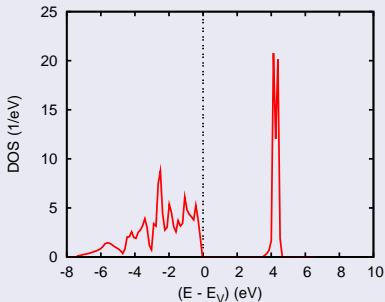
GGA: ≈ 3.5 eV,

exp.: 5.6 eV

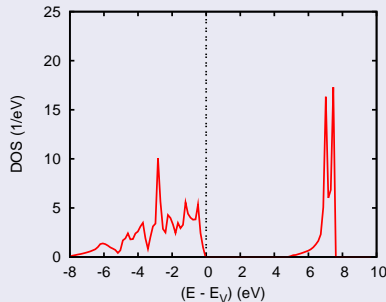


LaAlO₃

GGA

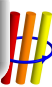


HSE



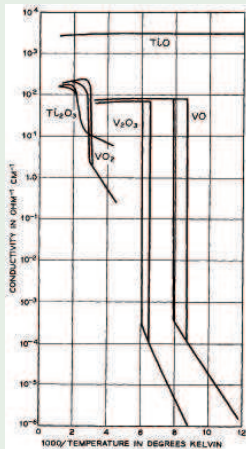
Bandgap

GGA: ≈ 3.5 eV, HSE: ≈ 5.0 eV, exp.: 5.6 eV



Metal-Insulator Transition of VO₂

Morin, PRL 1959



Metal-Insulator Transitions (MIT)

- VO₂ (d^1)
 - 1st order, 340 K, $\Delta\sigma \approx 10^4$
 - rutile \rightarrow M₁ (monoclinic)
- V₂O₃ (d^2)
 - 1st order, 170 K, $\Delta\sigma \approx 10^6$
 - corundum \rightarrow monoclinic
 - paramagn. \rightarrow AF order

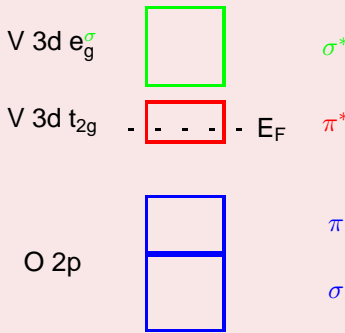
Origin of the MIT???

- Structural Changes?
- Electron Correlations?



Metal-Insulator Transition of VO₂

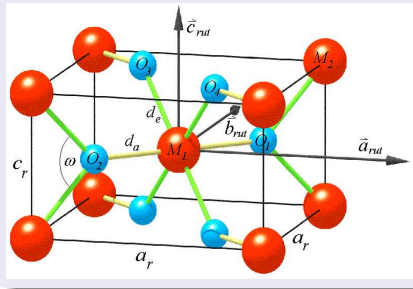
Octahedral Coordination



- V 3d-O 2p hybridization
 - σ , σ^* ($p-de_g^\sigma$)
 - π , π^* ($p-dt_{2g}$)

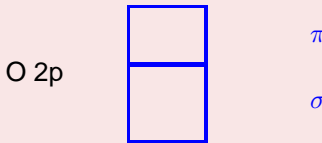
Rutile Structure

- simple tetragonal
- P4₂/mnm (D_{4h}¹⁴)



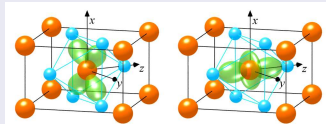
Metal-Insulator Transition of VO₂

Octahedral Coordination

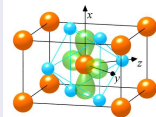
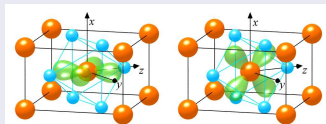


- V 3d-O 2p hybridization
 - σ , σ^* ($p-de_g^\sigma$)
 - π , π^* ($p-dt_{2g}$)

e_g^σ Orbitals

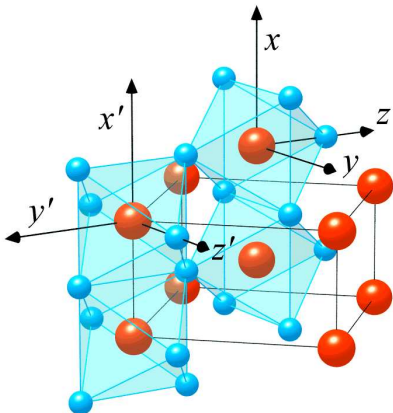


t_{2g} Orbitals



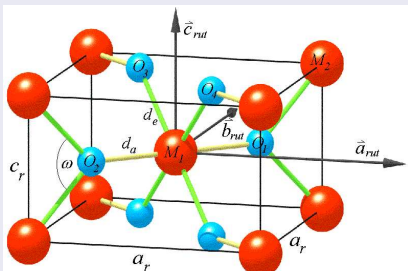
Metal-Insulator Transition of VO₂

Octahedral Chains



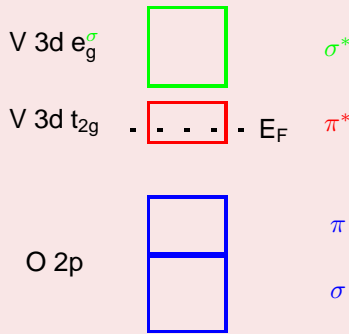
Rutile Structure

- simple tetragonal
- P4₂/mnm (D_{4h}^{14})

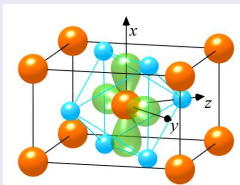
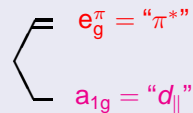
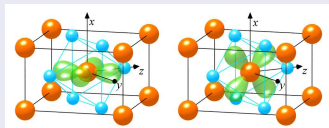


Metal-Insulator Transition of VO₂

Octahedral Coordination

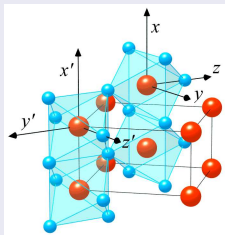


t_{2g} Orbitals

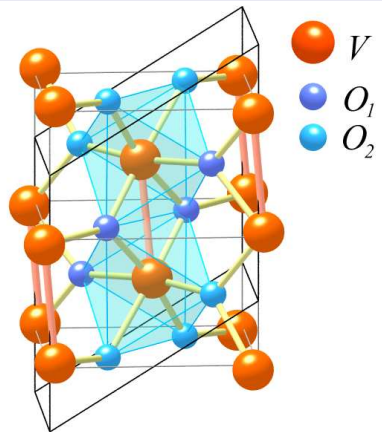


Metal-Insulator Transition of VO₂

Rutile Structure



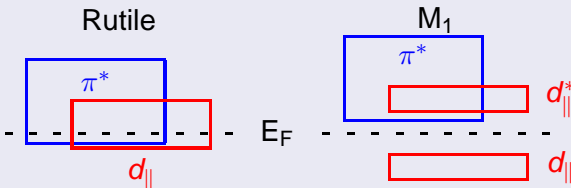
M₁-Structure



Structural Changes

- V-V dimerization $\parallel c_R$
- antiferroelectric displacement $\perp c_R$

Metal-Insulator Transition of VO₂

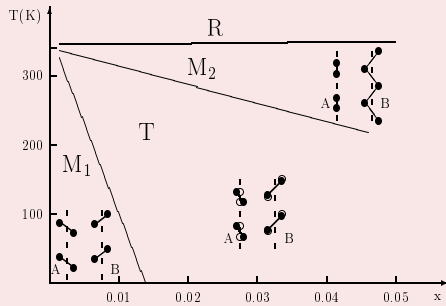


- Goodenough, 1960-1972
 - metal-metal dimerization $\parallel c_R \rightarrow$ splitting into d_{\parallel} , d_{\perp}^*
 - antiferroelectric displacement $\perp c_R \rightarrow$ upshift of π^*
 - Zylbersztein and Mott, 1975
 - splitting of d_{\parallel} by electronic correlations
 - upshift of π^* unscreened d_{\parallel} electrons



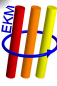
Metal-Insulator Transition of VO₂

Other Phases



- doping with Cr, Al, Fe, Ga
- uniaxial pressure $\parallel \langle 110 \rangle$

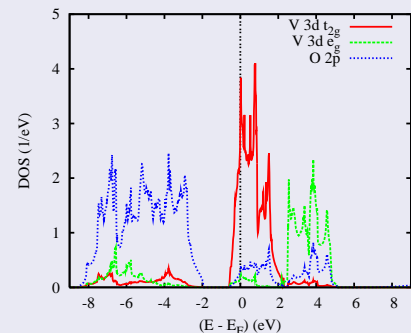
$\text{Cr}_x\text{V}_{1-x}\text{O}_2$
Pouget, Launois, 1976



Electronic Structure in Detail

Rutile Structure

- molecular-orbital picture ✓
- octahedral crystal field
 $\Rightarrow \text{V } 3d \ t_{2g}/e_g$
- V 3d–O 2p hybridization



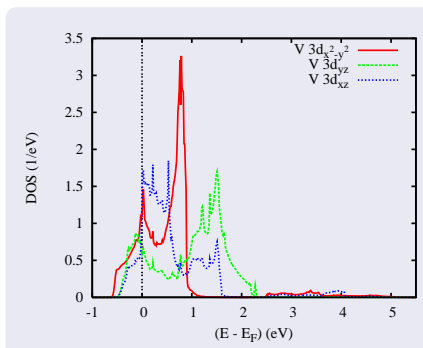
Ann. Phys. (Leipzig) 11, 650 (2002)



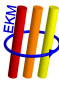
Electronic Structure in Detail

Rutile Structure

- molecular-orbital picture ✓
- octahedral crystal field
 $\Rightarrow V\ 3d\ t_{2g}/e_g$
- $V\ 3d$ -O $2p$ hybridization
- t_{2g} at E_F : $d_{x^2-y^2}$, d_{yz} , d_{xz}
- $n(d_{x^2-y^2}) \approx n(d_{yz}) \approx n(d_{xz})$

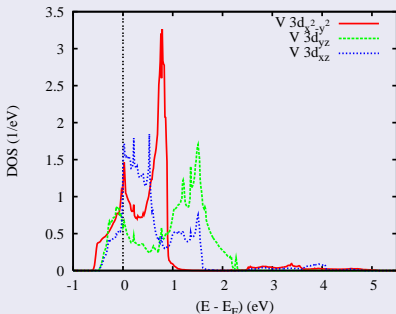


Ann. Phys. (Leipzig) 11, 650 (2002)

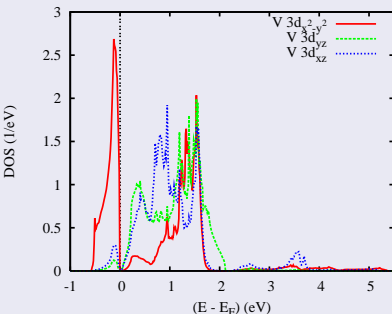


Electronic Structure in Detail

Rutile Structure



M₁ Structure



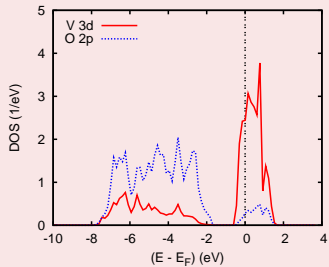
- bonding-antibonding splitting of d_{\parallel} bands
- energetical upshift of π^* bands \Rightarrow orbital ordering
- optical band gap on the verge of opening



New Calculations: GGA vs. HSE

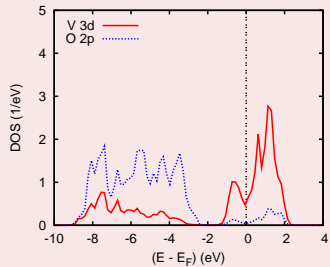
Rutile Structure

GGA



Rutile Structure

HSE



Rutile Structure: GGA \Rightarrow HSE

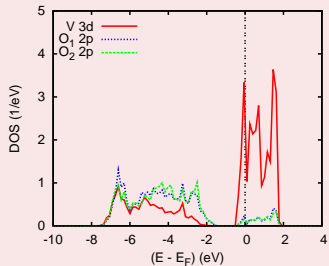
- broadening of O 2p and V 3d t_{2g} (!) bands
- splitting within V 3d t_{2g} bands



New Calculations: GGA vs. HSE

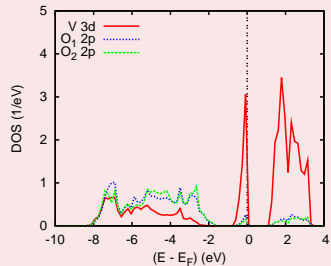
M₁ Structure

GGA



M₁ Structure

HSE

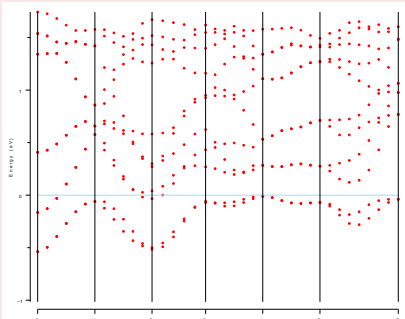


M₁ Structure: GGA \Rightarrow HSE

- splitting of d_{\parallel} bands, upshift of π^* bands
- optical bandgap of ≈ 1 eV

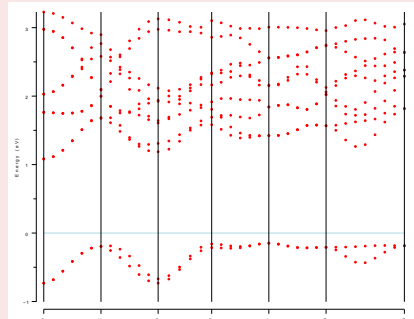
New Calculations: GGA vs. HSE

M₁ Structure



GGA

M₁ Structure



HSE

M₁ Structure: GGA \Rightarrow HSE

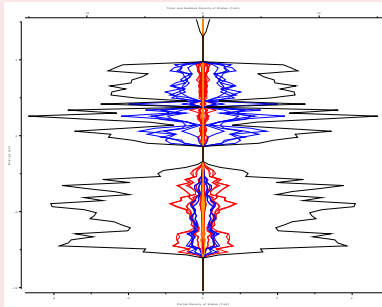
- splitting of d_{\parallel} bands, upshift of π^* bands
- optical bandgap of ≈ 1 eV



New Calculations: GGA vs. HSE

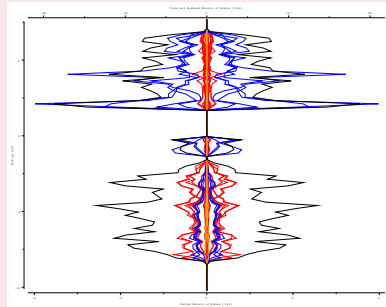
M₂ Structure

GGA



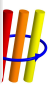
M₂ Structure

HSE



M₂ Structure: GGA \Rightarrow HSE

- localized magnetic moment of $1 \mu_B$
- optical bandgap of ≈ 1.6 eV



Unified Picture

Rutile-Related Transition-Metal Dioxides

VO_2 ($3d^1$), NbO_2 ($4d^1$), MoO_2 ($4d^2$)
(WO_2 ($5d^2$), TcO_2 ($4d^3$), ReO_2 ($5d^3$))

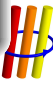
- instability against similar local distortions
 - metal-metal dimerization $\parallel c_R$
 - antiferroelectric displacement $\perp c_R$
- („accidental“) metal-insulator transition of the d^1 -members

VE *et al.*, J. Phys.: CM **12**, 4923 (2000)

VE, Ann. Phys. **11**, 650 (2002)

VE, EPL **58**, 851 (2002)

J. Moosburger-Will *et al.*, PRB **79**, 115113 (2009)

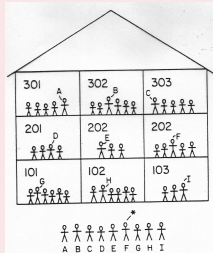


Success Stories

Basics

- DFT (exact, ground state)
- LDA, GGA, ...

Percus-Levy partition



Success Stories

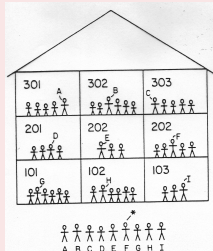
Basics

- DFT (exact, ground state)
- LDA, GGA, ...

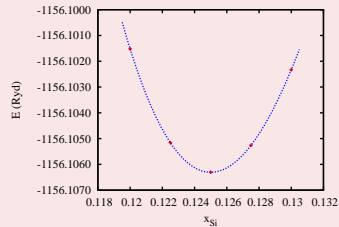
Implementation

- Muffins and beyond
- Full-Potential ASW

Percus-Levy partition



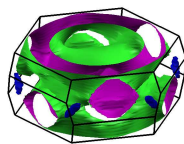
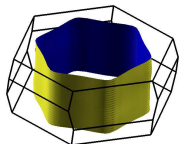
Full-Potential Code



Success Stories

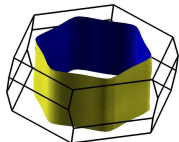
Delafoossites

2D → 3D

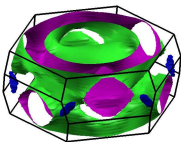


Success Stories

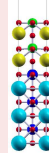
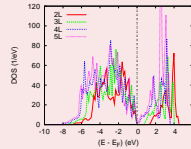
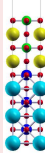
Delafoossites



2D → 3D



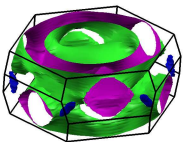
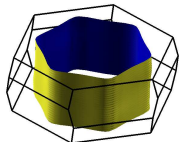
LaAlO₃/SrTiO₃



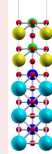
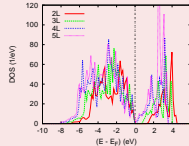
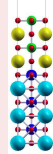
Success Stories

Delafoossites

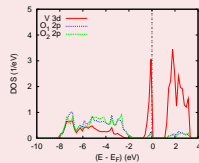
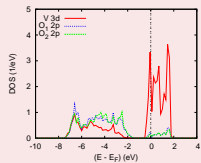
2D → 3D



LaAlO₃/SrTiO₃

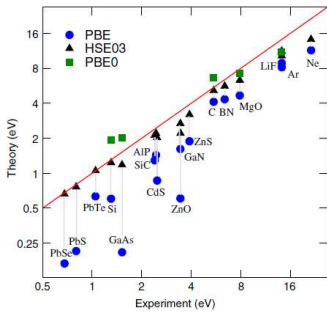


Metal-Insulator Transitions in VO₂

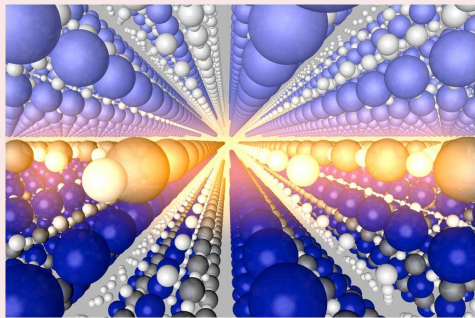


Visions

Methods



Materials



Acknowledgments

Augsburg

M. Breitschaft, U. Eckern,
K.-H. Höck, S. Horn, R. Horny,
T. Kopp, J. Kündel, J. Mannhart,
J. Moosburger-Will, N. Pavlenko,
W. Scherer, D. Vollhardt

TRR 80



Caen

R. Frésard,
S. Hébert,
A. Maignan,
C. Martin

Darmstadt/Jülich

P. C. Schmidt, M. Stephan,
J. Sticht †

Europe/USA

E. Wimmer, A. Mavromaras,
P. Saxe, R. Windiks, W. Wolf



Acknowledgments

Augsburg

M. Breitschaft, U. Eckern,
K.-H. Höck, S. Horn, R. Horny,
T. Kopp, J. Kündel, J. Mannhart,
J. Moosburger-Will, N. Pavlenko,
W. Scherer, D. Vollhardt

TRR 80



Caen

R. Frésard,
S. Hébert,
A. Maignan,
C. Martin

Darmstadt/Jülich

P. C. Schmidt, M. Stephan,
J. Sticht †

Europe/USA

E. Wimmer, A. Mavromaras,
P. Saxe, R. Windiks, W. Wolf

Würzburg

Thank You for Your Attention!

